

Regular Article

Adsorption and insertion of polyarginine peptides into membrane pores: The trade-off between electrostatics, acid-base chemistry and pore formation energy



Pedro G. Ramírez^a, Mario G. Del Pópolo^b, Jorge A. Vila^a, I. Szleifer^d, Gabriel S. Longo^{c,*}

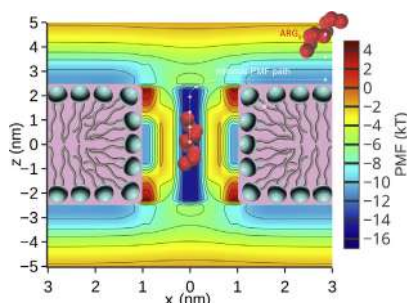
^a Instituto de Matemática Aplicada San Luis (IMASL), UNSL-CONICET, San Luis, Argentina

^b IICB-CONICET & Facultad de Ciencias Exactas y Naturales (FCEN), UNCuyo, Mendoza, Argentina

^c Instituto de Investigaciones Fisicoquímicas Teóricas y Aplicadas (INIFTA), UNLP-CONICET, La Plata, Argentina

^d Department of Biomedical Engineering, Department of Chemistry and Chemistry of Life Processes Institute, Northwestern University, Evanston IL, USA

GRAPHICAL ABSTRACT



ARTICLE INFO

Article history:

Received 22 March 2019

Revised 24 May 2019

Accepted 25 May 2019

Available online 30 May 2019

Keywords:

Cell penetrating peptides

Molecular modeling

ABSTRACT

The mechanism that arginine-rich cell penetrating peptides (ARCPPs) use to translocate lipid membranes is not entirely understood. In the present work, we develop a molecular theory that allows to investigate the adsorption and insertion of ARCPPs on membranes bearing hydrophilic pores. This method accounts for size, shape, conformation, protonation state and charge distribution of the peptides; it also describes the state of protonation of acidic membrane lipids. We present a systematic investigation of the effect of pore size, peptide concentration and sequence length on the extent of peptide adsorption and insertion into the pores. We show that adsorption on the intact (non-porated) lipid membrane plays a key role on peptide translocation. For peptides shorter than nona-arginine, adsorption on the intact membrane increases significantly with chain length, but it saturates for longer peptides. However, this adsorption behavior only occurs at relatively low peptide concentrations; increasing peptide concentration favors adsorption of the shorter molecules. Adsorption of longer peptides increases the intact membrane negative charge as a result of further deprotonation of acidic lipids. Peptide insertion into the pores depends non-monotonically on pore radius, which reflects the short range nature of the effective membrane-peptide interactions. The size of the pore that promotes maximum adsorption depends on the peptide chain length. Peptide translocation is a thermally activated process, so we complement our thermodynamic approach with a simple kinetic model that allows to rationalize the ARCPPs translocation rate in terms of the free energy gain of adsorption, and the energy cost of creating a transmembrane pore with peptides in it. Our results indicate that strategies to improve translocation efficiency should focus on enhancing peptide adsorption.

© 2019 Elsevier Inc. All rights reserved.

* Corresponding author.

E-mail address: longogs@inifta.unlp.edu.ar (G.S. Longo).

1. Introduction

In the context of cell biology, lipid bilayers act as semi-permeable barriers separating aqueous compartments. Membranes' selective permeability is a key feature that allows organisms to establish vital concentration gradients between the intra- and extra-cellular media. Most lipids in membrane bilayers are amphipathic molecules, arranged with their polar heads pointing outwards, which creates a hydrophobic region inside the bilayer. This region is impermeable to most hydrophilic molecules, thereby acting as a protective wall that encloses the cellular matrix. Essential small molecules such as ions, sugars and amino acids can traverse the plasma membrane through the action of protein pumps and channels embedded in the membrane [1]. Biological membranes host proteins that function as ligand-receptor gateways to permit transport and other functions [2]. Most polar and hydrophilic bioactive molecules that lack a proper surface receptor, find in lipid membranes an impermeable barrier.

Certain peptide sequences, however, are capable of penetrating lipid bilayers. Cell penetrating peptides (CPPs) are short sequences of amino acids (≤ 30) that enter most mammalian cells. These molecules can penetrate into cells either alone or attached to cargoes of various sizes such as fluorescent probes, proteins, oligonucleotides and liposomes [3–17], which has raised interest in their possible application as vehicles for intra-cellular delivery of therapeutic agents [18,19].

The first CPP described in the literature was the arginine-rich sequence of the transduction domain of the HIV-1 transactivator of transcription (TAT) protein, identified as key to facilitate cellular uptake of the TAT protein [20]. This discovery jump-started the scientific community's interest in the use of arginine-rich cell penetrating peptides (ARCPPs) as drug delivery carriers. Nowadays, there is considerable interest within the therapeutic peptides industry in developing reliable carriers for delivery to the cellular cytoplasm [21,22]. Many CPPs are highly polar and hydrophilic, which poses fundamental questions as to the mechanism by which they traverse lipid bilayers. Understanding the physical chemistry underneath this mechanism is essential for the rational design of drug delivery vehicles with controlled behavior based on the CPPs' ability to enter cells.

Polyarginine peptides display higher translocation efficiency than other cationic CPPs such as polylysine and TAT peptides [4,7,8,11,12,23]. Most studies agree that the cell-penetrating properties of these peptides originate from the positively charged amino acids within their sequence [24–26], and the concomitant electrostatic interaction with the negatively charged membrane surface [6,27–31].

Different mechanisms have been proposed to describe the cellular uptake of CPPs [1,14,15,32,33]. They can be internalized through endocytosis, and can also cross the membrane through direct translocation when endocytosis is inhibited [33–36]. Direct translocation was first questioned as an artifact of cell fixation, but it was later confirmed using fluorescence microscopy in living cells when other uptake routes are inhibited [12]. Indeed, there is evidence that CPPs' uptake is independent of metabolic energy and does not involve any specific cell receptor [24,37–39]. As opposed to the endocytic pathway, direct translocation does not require the input of metabolic energy. After years of intense debate, it is now accepted that both energy-dependent and energy-independent mechanisms account for the cell permeation properties of CPPs [15].

Various models of direct translocation have been proposed [15,40–45], the most accepted one requiring the opening of hydrophilic transmembrane pores [46,47]. However, at the present, the exact physical pathway that CPPs use to passively cross lipid bilayers is only partially understood [48,49]. Although, there is growing

consensus that peptides' adsorption on the cell membrane plays a critical role during the initial stages of permeation.

It should be noted that while originally most identified CPPs were of cationic nature, there is currently an increasing number of synthetic CPPs that contain mostly hydrophobic amino acids while having a relatively low net electric charge. The amphipathic nature of these peptides plays a crucial role in their ability to interact with the lipid membrane, which may result in internalization mechanisms different from direct translocation [50].

Theory and molecular simulations have been used to shed light on the underlying mechanism of CPP uptake, including molecular dynamics (MD) with both all-atom and coarse-grained models [46,47,51–56]. The effect of membrane tension on the uptake [53] and translocation through asymmetric membranes [51] have both been considered. By use of MD simulations, Via et al. [47] have recently shown that the transmembrane potential can significantly lower the energy barrier for bringing the CPP to the center of the bilayer. Ziegler et al. [27] have demonstrated that the electrostatic energy of peptide-membrane attractions, calculated within the Gouy-Chapman formalism, accounts for approximately 80 percent of the binding energy.

While plenty of advances have been made to elucidate the mechanisms of direct translocation, there are still many questions that need to be answered. For example, what is the role of membrane composition, its surface charge and in particular the state of protonation of acidic lipids? Moreover, ARCPPs translocate more efficiently when they have between 8 and 15 residues [57]. Wender et al. [25] highlighted nona-arginine (ARG_9) as the most efficient CPP that is composed of natural L-amino acids. Why do these different ARCPPs show different translocation efficiencies? In other words, what is the role of peptide chain-length, net charge and conformational flexibility?

To address these questions, we have developed a molecular-level theory that describes the equilibrium adsorption of polyarginine peptides on lipid bilayers bearing a transmembrane hydrophilic pore. This theory explicitly accounts for the acid-base equilibrium of all titratable species, the electrostatic and steric interactions as well as entropic effects, while also incorporating specific molecular information of the peptides, including size, shape, conformation, protonation state, and charge distribution. The state of protonation of lipids in the membrane and that of individual peptide residues are not assumed a priori but predicted locally depending on the interplay between molecular organization and the aforementioned free energy contributions. In this work, we present a systematic study of the effect of pore radius and CPP chain-length and concentration on the interaction of these peptides with porated and intact (non-porated) membranes.

While peptide adsorption on the intact and porated membrane can be studied using a thermodynamic approach, passive peptide translocation involves the nucleation of a transmembrane pore, which is a thermally activated process. We conclude this work by presenting a simple kinetic model where CPP translocation rate is described in terms of three couple first-order stages: (i-ii) peptide adsorption/desorption on/from the intact membrane, and (iii) activated jump of the peptide across the lipid bilayer. The resulting membrane translocation rate depends on two thermodynamic parameters, the adsorption and activation free energies, that can be evaluated using the equilibrium molecular theory derived in this work.

2. Method: Theory and molecular model

The system under investigation is sketched in Fig. 1; it is composed of a lipid membrane having a pore connecting two regions of

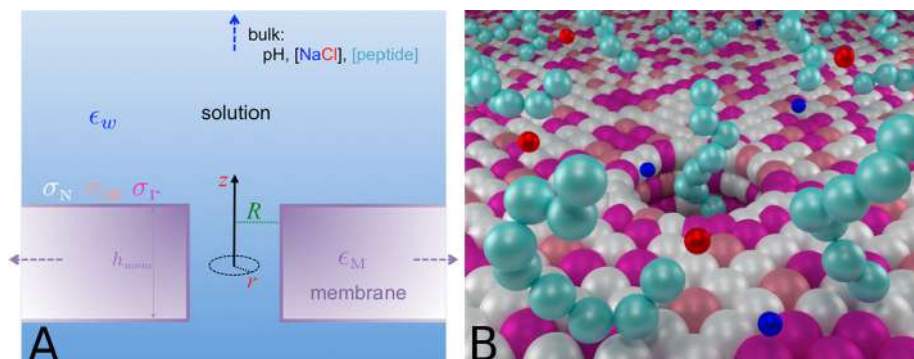


Fig. 1. Schematic representations of the system. Panel A illustrates a longitudinal cut of the system. Panel B shows a 3D representation of a top-down view of the hydrophilic membrane pore and its surroundings. The color of each sphere in panel B indicates its chemical identity, following the same color-scheme of panel A. (For interpretation of the references to color in this figure legend, the reader is referred to the web version of this article.)

an aqueous solution that contains arginine peptides (P), water molecules (w), hydroxyl ions (OH^-), hydronium ions (H^+) and monovalent salt ($NaCl$) anions ($-$) and cations ($+$). The membrane is composed of a mixture of two types of lipids, a charge neutral one (N) and another one bearing an acidic group (I); this ionizable lipid can be found in one of two possible chemical states: either protonated (charge neutral, IH) or deprotonated (negatively charged, I^-). In the following we summarize the most important details of this theoretical method, while a full description of the theory is presented in the [Electronic Supplementary Information \(ESI\)](#).

The first step in our thermodynamic approach consists of writing all the different contributions to the total Helmholtz free energy of the system:

$$F = -TS_{TF} - TS_{TP} + F_{CP} + F_{MS} + U_E \quad (1)$$

where T is the temperature, S_{TF} represents the translational entropy of all free species but the peptide, including water molecules, hydronium, hydroxide, and salt ions. The translational and conformational entropy of the peptide is S_{TP} , and F_{CP} is the chemical free energy of these molecules, which accounts for the acid-base equilibrium of the titratable side chain of arginine residues. The surface free energy is F_{MS} , which describes the non-electrostatic free energy contributions from the membrane, including the acid-base equilibrium of the ionizable lipid. Since the membrane is in its liquid disordered phase, this term also includes the translational entropy of the lipids. Lastly, U_E is the electrostatic energy.

Each of the terms that make the free energy can be explicitly written as a functional of a few position-dependent quantities, comprising (i) the local densities of all the mobile species in the solution, including peptide and lipids (ii) the local probability of different conformations of the peptide, (iii) the local degree of protonation of each titratable unit, and (iv) the electrostatic potential. The next step is to optimize the thermodynamic potential with respect to each of these functions, which allows to express them in terms of only two local interaction potentials: the osmotic pressure and the electrostatic potential. These interaction potentials can be calculated through a series of non-linear coupled equations, which are solved numerically.

These equations are the Poisson equation, the incompressibility constraint of the fluid solution, which requires every element of volume to be fully occupied by some of the mobile species, and the incompressibility of the membrane surface, which requires every area element to be fully occupied by lipids. These equations are derived self-consistently within the present method. Once the local interaction potentials are calculated, functions (i) to (iv) and, consequently, the total free energy are all known. Any thermodynamic quantity of interest can be derived from the minimized free

energy. In addition, structural properties of the peptides can be calculated using their local density and probability distribution of its different conformations.

The system is in chemical equilibrium with a bulk solution, whose composition far away from the membrane (pH, salt and peptide concentrations) is controlled. The membrane composition far from the pore is also controlled. Thus, the proper thermodynamic potential whose minimum yields the equilibrium conditions is the semi-grand potential, which is a function of the chemical potentials of both the solution species and the lipids.

In order to apply this theory, we need to define a molecular model for the peptide and the lipid membrane. We model the membrane interior as a region with dielectric permittivity $\epsilon_M = 2$; solution molecules are excluded from this region, which is given by

$$r > R \text{ and } -\frac{h_{mem}}{2} < z < \frac{h_{mem}}{2} \quad (2)$$

where R is the radius of the cylindrical pore and h_{mem} is the membrane thickness. The pore center gives the origin of our cylindrical coordinate system, $(r, z) = (0, 0)$. The upper ($z = \frac{h_{mem}}{2}$ and $r \geq R$) and lower ($z = -\frac{h_{mem}}{2}$ and $r \geq R$) membrane surfaces are planar. Then, the system is symmetric over the $z=0$ plane, and we also impose reflexion symmetry with respect to the $z=0$ plane. Thus, we will only present results for $z \geq 0$.

On the membrane surface, the local area density of the lipids is $\sigma_N(S)$ for the neutral lipid and $\sigma_I(S)$ for the ionizable lipid, where S is a coordinate on the membrane surface. This coordinate is equal to z on the cylindrical surface of the pore and equal to the displaced radial coordinate on the planar membrane surface, to make S continuous,

$$S = \begin{cases} z & 0 \leq z < \frac{h_{mem}}{2} \text{ when } r = R \\ r - R + \frac{h_{mem}}{2} & r \geq R \text{ when } z = \frac{h_{mem}}{2} \end{cases} \quad (3)$$

The area fractions of membrane surface occupied locally by each lipid are $\chi_N(S) = \sigma_N(S)a_N$ and $\chi_I(S) = \sigma_I(S)a_I$ for the neutral and acidic species respectively, where $a_N = 0.6 \text{ nm}^2$ and $a_I = 0.6 \text{ nm}^2$ are the area per molecule (or head-group).

Far away from the pore ($S \rightarrow \infty$), the lipid composition is controlled, which implies that $\chi_N^\infty = \lim_{S \rightarrow \infty} \chi_N(S)$ and $\chi_I^\infty = \lim_{S \rightarrow \infty} \chi_I(S)$ are input variables. Typically, anionic lipids account for less than half of the phospholipids in biological membranes [58,59] and 3:1 neutral:ionic lipid ratios are often used in model membrane studies [60,61]; we use lipid area fractions of $\chi_N^\infty = 0.6$ and $\chi_I^\infty = 0.4$ for the neutral and ionizable lipids respectively. For the ionizable lipid $pK_a = 4$, representing a fatty acid, and the local degree of charge is $f_{I^-}(S)$. The area density of charged lipid

is $\sigma_I(S) = \sigma_I(S)f_I(S)$, and that of the protonated lipid $\sigma_{IH}(S) = \sigma_I(S)(1 - f_I(S))$. Notice that $\sigma_I(S)$ also gives the area charge density of the membrane surface. We emphasize again that we do not impose the degree of charge of the lipids on the basis of its pK_a and the solution's pH; rather, $f_I(S)$ results from the local conditions that yield thermodynamic equilibrium.

Polyarginine molecules are modeled as interconnected beads of volume $v_{ARG} = 0.21 \text{ nm}^3$, which is the apparent molar volume of arginine as reported by Millero et al. [62]; each bead is centered at the C_α position with a basic $pK_a = 12$. All conformations of the peptide chain are generated using a rotational isomeric state model in which each 0.38 nm long segment can assume one of three isoenergetic orientations [63]. To account for the rotational degrees of freedom, each of these conformations is rotated 12 times according to randomly selected Euler angles.

Other inputs of our molecular model are the volume (and charge) of the rest of the free species; for water molecules, hydronium and hydroxide ions we use 0.03 nm^3 , and the volume of salt ions is 0.045 nm^3 . The aqueous medium has dielectric constant $\epsilon = \epsilon_w \epsilon_0$, with $\epsilon_w = 78.5$ being the relative dielectric constant of water at room temperature, and ϵ_0 denoting the vacuum permittivity. In order to numerically solve the equations resulting from the molecular theory, the space is discretized into 0.25 nm-thick and 0.5 nm-wide cylindrical rings. The area of the different membrane surfaces (membrane-solution interfaces) is discretized accordingly.

3. Results

In this work, we present theoretical results for the adsorption at physiological conditions of short polyarginine peptides on lipid membranes bearing pores of different size. We will show that far away from the pore, where the membrane properties are those of the intact membrane, peptides attach quite strongly to the membrane surface. Our results predict this behavior for all peptide sizes and pore radii considered, which highlights the critical role of adsorption as a mechanistic first stage on the direct translocation pathway.

Therefore, before considering the effect of pore size, we describe the thermodynamics of adsorption of polyarginines on the surface of a membrane having no pore. To quantify this behavior, we define the adsorption on the intact membrane as the number of peptide molecules per unit area in excess of the bulk contribution,

$$\Gamma_{mem} = \int_0^\infty dz (\langle \rho_p(z) \rangle - \rho_p^b) \quad (4)$$

where ρ_p^b and $\langle \rho_p(z) \rangle$ are the bulk and the local peptide number density, such that

$$\lim_{z \rightarrow \infty} \langle \rho_p(z) \rangle = \rho_p^b \quad (5)$$

Angle brackets indicate ensemble average over peptide conformations.

Fig. 2 shows the surface excess of arginine peptides with different chain lengths (L). These and all the following results correspond to physiological conditions (pH7 and 0.1 M NaCl) and a bulk concentration of polyarginine of $1 \mu\text{M}$; the membrane is composed of 40% ionizable lipid and 60% electroneutral lipid, and its thickness is $h_{mem} = 5 \text{ nm}$. The inset in Fig. 2 displays the area charge density, σ_I , that establishes at the intact membrane surface once adsorption equilibrium has been attained.

Increasing the polyarginine chain-length dramatically enhances adsorption, as seen in Fig. 2, and Γ_{mem} displays a seemingly asymptotic behavior for relatively long peptides. Indeed, peptides longer than ARG₉ only marginally increase the saturation surface excess to

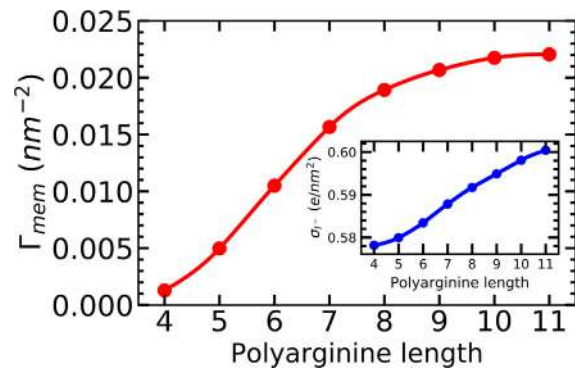


Fig. 2. Peptide surface excess, Γ_{mem} , on the intact membrane as a function of peptide chain length, from $L = 4$ to $L = 11$. The inset displays the area charge density of the intact membrane surface, σ_I , as a function of polyarginine chain length. These results correspond to physiological conditions (pH 7 and 0.1 M NaCl) and an experimentally relevant peptide concentration of $1 \mu\text{M}$.

the intact lipid membrane. This predictions, together with the critical role of peptide adsorption to the intact membrane, must be both placed in the context of the findings of Wender et al. [25], which indicate that ARG₉ is one of the most efficient CPP composed of natural L-amino acids.

However, though the number of adsorbed molecules may be similar for $L \geq 9$, longer peptides still bring more positive charge to the surface. For this reason, the negative charge density on the membrane surface does not display the same asymptotic behavior as Γ_{mem} (see inset of Fig. 2). This monotonic increase in surface charge is the result of a lower degree of protonation of acidic lipids as the peptide length increases.

Physical binding to the membrane surface is driven by the electrostatic attraction between the negatively charged lipids and the positively charged arginine residues. The release of salt counterions to the bulk solution favors adsorption, although this phenomenon should only play a minor role at the high salt concentration used in our calculations (0.1 M) [64]. The loss of peptide translational entropy opposes adsorption. Confinement of longer peptides brings more electric charge (per molecule) to the surface at the same (translational) entropic cost as the adsorption of smaller molecules. This explains why adsorption increases more significantly with peptide size for intermediate chain lengths, $4 \leq L < 9$. Steric and electrostatic repulsions among adsorbed peptides, however, become larger as the size of the molecules increases. In addition, the peptide loss of conformational entropy (as opposed to translational entropy) is greater as the size of the molecule increases. These effects contribute to the saturation behavior observed when $L \geq 9$.

Next, we consider the effect of peptide concentration on its adsorption to the intact membrane. Fig. 3 shows adsorption isotherms, Γ_{mem} vs. peptide concentration, for three representative chain lengths. These adsorption isotherms saturate at around 0.01 M peptide. Further increasing the bulk concentration beyond this saturation value decreases Γ_{mem} . Clearly, longer peptides adsorb better at low concentrations, while shorter ones are more efficient at high peptide concentrations. A similar behavior has been predicted using MD simulations in a system comprised of a 1,2-Dipalmitoyl-sn-glycero-3-phosphocholine (DPPC) bilayer with cationic antimicrobial peptides having +4 and +7 charges; López Cascales et al. [65] found that peptides with a charge of +4 display a higher level of adsorption to the DPPC membrane than peptides with +7 charge. The theoretical model developed in this work does not allow for any type of membrane deformation or rupture; as such, we work under the assumption that the peptide concentrations explored do not break the intact membrane. Although our

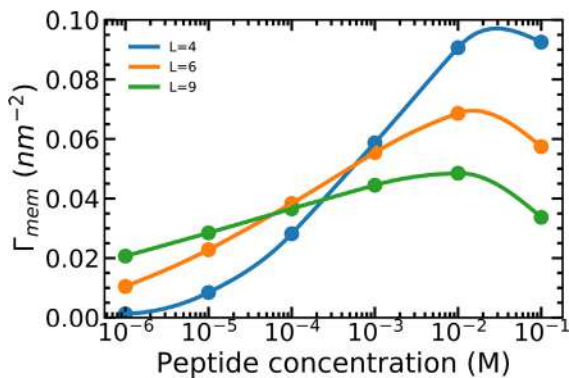


Fig. 3. Peptide surface excess, Γ_{mem} , on the intact membrane as a function of the bulk peptide concentration for three different chain lengths. These results were obtained at physiological conditions (pH 7 and 0.1 M NaCl).

theory can describe lipid translation and protonation, other theoretical/simulation methods such as Molecular Dynamics may be better suited to study membrane deformation due to peptide adsorption.

The effective interaction between the peptide and the membrane surface can be quantified using the potential of mean force, defined as (see ESI):

$$PMF(z) = -\ln \frac{\langle \rho_p(z) \rangle}{\rho_p^b} \quad (6)$$

where we have arbitrarily chosen $\lim_{z \rightarrow \infty} PMF(z) = 0$.

Fig. 4 shows the position-dependent PMF acting on a peptide with center of mass at z . Long polyarginines interact more strongly with the membrane surface. In particular, at the surface ($z = \frac{h_{mem}}{2}$), the PMF decreases monotonically with peptide size, as seen in the inset of Fig. 4. This last result is consistent with the predictions of Fig. 2 showing increasing adsorption with peptide size. At the conditions of our calculations, physiological pH and salt concentration, membrane-peptide interactions are short-ranged (*i.e.*, screened). Further than approximately 3 nm from the membrane surface, $PMF(z)$ nearly vanishes.

At the surface, the interaction between ARG₉ and the intact membrane surface is approximately $-11k_B T$ (see Fig. 4). By use of MD simulations, Hu and Patel [54] have obtained a similar result for the interaction between TAT peptides containing +8 charges

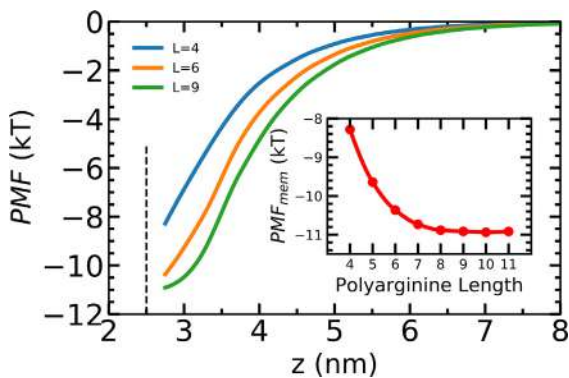


Fig. 4. Potential of mean force acting on peptides of three different chain lengths (L) as a function of the distance to the intact membrane surface. The surface sits at $z = \frac{h_{mem}}{2} = 2.5$ nm, indicated by the dashed black line. The inset shows the PMF value at the membrane surface, PMF_{mem} , as a function of the polyarginine chain length. These results were obtained at physiological conditions (pH 7 and 0.1 M NaCl) and an experimentally relevant peptide concentration of 1 μ M.

and a 50:50 DPPC:DPPS (1,2-dipalmitoyl-sn-glycero-3-phospho-L-serine) membrane.

As stated before, molecular simulations and experimental evidence support the hypothesis that CPPs translocate lipid bilayers by nucleating transient membrane pores. Consequently, we now turn our attention to peptide adsorption on lipid membranes having a pore of radius R . The pore breaks the symmetry on the planes normal to the z -direction; we consider azimuthal symmetry and introduce the radial (polar) coordinate r . The center of the pore defines the origin of our cylindrical coordinate system. In this context, we define the pore adsorption extent as

$$\Gamma_{pore} = 2\pi \int_0^\infty dz \int_0^\infty r dr (\langle \rho_p(r, z) \rangle - \lim_{r \rightarrow \infty} \langle \rho_p(r, z) \rangle) \quad (7)$$

which measures the number of peptide molecules in excess of the number adsorbed on the intact membrane, given by the double integral of the second term. The intact membrane represents the boundary condition of the porated membrane, such that:

$$\lim_{r \rightarrow \infty} \langle \rho_p(r, z) \rangle = \langle \rho_p(z) \rangle \quad (8)$$

Notice that the peptide bulk density is also a boundary condition that satisfies $\rho_p^b = \lim_{z \rightarrow \infty} \langle \rho_p(r, z) \rangle = \lim_{z \rightarrow \infty} \langle \rho_p(z) \rangle$. Then, Γ_{pore} isolates the pore and the contribution from its surroundings to adsorption, while excluding the effect of the intact membrane.

Fig. 5 shows that Γ_{pore} displays a non-monotonic behavior as the pore size increases, with a maximum whose magnitude and position (R_{max}) depends on the peptide size. Long peptides concentrate more into the pore because they bring more positive charge to its surface, which enhances the attractive interactions with the negative charge of the pore, at the same (translational) entropy penalty due to molecular confinement. For small radii, as the size of the pore increases, there is more room for peptides to adsorb but also more net negative charge on the surface, which increases adsorption.

The non-monotonic behavior as the size of the pore increases is not completely unexpected since Γ_{pore} is an excess quantity with respect to the extent of adsorption on the intact planar surface. In the ESI, we show that Γ_{pore} diverges to negative values when $R \rightarrow \infty$. While the membrane area added to the pore surface grows linearly with R , the area removed to the planar surface decreases proportionally to R^2 . Namely, increasing the pore size for sufficient large R , removes more surface than it adds. Such decrease in surface area available for adsorption accounts for the behavior of Γ_{pore} for relatively large pore sizes.

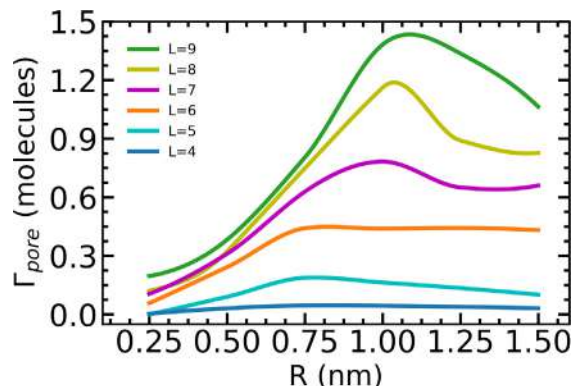


Fig. 5. Number of peptide molecules adsorbed to the pore, Γ_{pore} , as a function of the pore radius for different peptide chain lengths, from $L = 4$ to $L = 9$. These results have been obtained at physiological conditions (pH 7 and 0.1 M NaCl) and an experimentally relevant peptide concentration of 1 μ M.

Let us now consider the effective interaction between the peptides and the porated membrane. As in the case of the intact membrane (Eq. (6)), we define the potential of mean force as:

$$PMF(r, z) = -\ln \frac{\langle \rho_p(r, z) \rangle}{\rho_p^b} \quad (9)$$

where we have again chosen $\lim_{z \rightarrow \infty} PMF(r, z) = 0$. Notice that this free-energy surface does not include the energy cost of creating the pore. This contribution, which makes the translocation of the peptide a thermally activated event, will be considered later.

Fig. 6 illustrates $PMF(r, z)$ for the adsorption of ARG₉ to a membrane having a pore of 1 nm radius. The upper membrane surface corresponds to $(z = \frac{h_{mem}}{2}, r > R)$, while the cylindrical pore surface is $(\frac{h_{mem}}{2} > z > -\frac{h_{mem}}{2}, r = R)$. In this figure the red line with circles represents the minimum free energy path that takes a peptide from the bulk solution into the membrane pore. The resulting reaction path highlights the role of peptide adsorption on the intact surface prior insertion into the membrane pore. Clearly, as z decreases, the peptide first approaches the surface far away from the pore, which is centered at $r = 0$. The peptide then attaches to the bilayer relatively far away from the pore, where the surface properties of the membrane are those of the intact membrane, which occurs at $r \rightarrow \infty$. This behavior is observed for all peptide sizes and pore radii considered.

To further characterize the effective interaction between the peptides and the porated membranes, Fig. 7 shows the potential of mean force for different chain lengths and pore sizes, calculated using Eq. (9). In all cases, $PMF(r, z)$ displays a local minimum on the membrane surface and a global minimum inside the pore. For short peptides and large pores this global minimum occurs relatively close to the pore surface (see panels A and C of Fig. 7). As the peptide size increases, or the pore radius decreases, the minimum displaces towards the pore center ($r = 0$).

In agreement with the behavior predicted for the intact membrane (see Fig. 2), the minimum of the PMF for porated membranes becomes deeper (more negative) the longer the arginine chain (e.g., in Fig. 7 compare different panels on the same column). Long peptides bring more counterion charge to the membrane surfaces at the same entropic cost of confinement. Moreover, the short-range nature of these effective interactions, seen in Fig. 7 for porated membranes, but also in Fig. 4 for the intact membrane, is the reason why the position of the PMF minimum (inside the

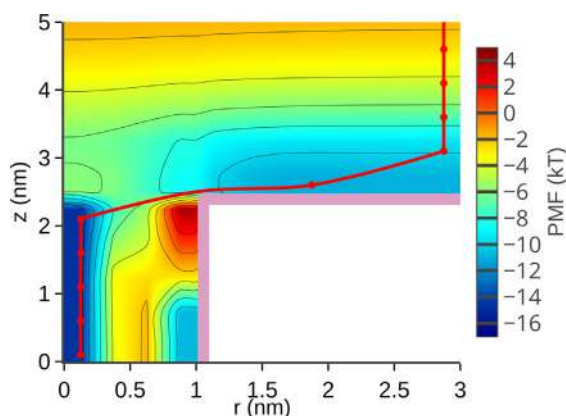


Fig. 6. The color map shows $PMF(r, z)$ for ARG₉ at different spatial positions (excluding the membrane interior where it diverges). The horizontal pink line corresponds to the upper membrane surface, while the vertical one represents the cylindrical surface of a 1 nm-radius pore. The red circles show the minimum free energy path on the $r - z$ plane. These results correspond to physiological conditions (pH 7 and 0.1 M NaCl) and peptide concentration 1 μ M. (For interpretation of the references to color in this figure legend, the reader is referred to the web version of this article.)

pore) displaces towards the pore surface, either as the size of the pore increases or as the peptide size decreases.

Fig. 7 also shows that the potential of mean force displays a local and global maximum near the edge of the pore; i.e., close to the border between the planar and the cylindrical surfaces but inside the pore. Peptide inclusion into the pore requires placing the peptide's segments close enough to one of the membrane surfaces, given that the effective interactions are short ranged. Indeed, the spatial distribution of peptide segments does not display such maximum (see ESI). In broad terms, placing the peptide center of mass in the vicinity of the maximum requires the molecule to assume an upright configuration, which leads to half of its segments insufficiently coordinated with the negatively charged lipids. This geometric restriction does not impose a significant constraint for adsorption on the planar side of the edge, which is why the maximum occurs in the pore interior. Moreover, as the size of the peptide increases the maximum grows because more segments are placed too far away from the membrane when the molecule center of mass is at this position.

The gray color scale in Fig. 7 shows the local charge density of the membrane, $\sigma_r(S)$, where S is a coordinate on the membrane surface as already defined. In these examples, the pore surface is more negatively charged than the planar membrane surface (as evidenced by the darker gray color). Our membrane is composed of a charge-neutral lipid and of a titratable lipid that can be found in one of two chemical states, either protonated (charge neutral) or deprotonated (negatively charged). Then, the observed charge regulation behavior inside the pore can either result from the exchange between neutral and (charged) ionizable lipids, or be associated to a lower degree of protonation of the ionizable lipid inside the pore.

Fig. 8 reports the local membrane composition for a selected set of conditions. The curves representing the total area fraction occupied by titratable lipids (green line) and that of charged lipids (red line) are roughly parallel to each other, indicating that protonated and deprotonated species do not segregate from each other and follow similar spacial distributions on the membrane. Charge density on the bilayer surface is proportional to the local area fraction occupied by ionized lipids. The results of Fig. 8 imply that the degree of protonation of the acidic lipids does not significantly depend on the position on the surface. On the other hand, the local area occupied by neutral and ionizable lipids change inside and near the pore, with respect to the planar surface, and assumes different values depending on the size of the pore. In our model, both ionizable and neutral lipid molecules occupy the same molecular area. Under such condition, the main contribution to membrane charge regulation is the exchange of lipid types inside and near the pore, as discussed. However, this behavior could be different for lipids having different area per molecule.

In Fig. 2 we have shown that the charge of the intact membrane surface increases as a function of the peptide chain length as a consequence of the increasing deprotonation of the ionizable lipids. Plots of membrane charge density at $S = 0$ as a function of both polyarginine length and pore radius are available in the ESI. Those plots show that the charge on the pore surface can significantly vary with the pore size. The main contribution to this charge regulation mechanism is the aforementioned exchange between charged and neutral lipids. The dependence on peptide size is much weaker.

Surface Plasmon Resonance studies have shown that incorporation of the CPP pep-1 is a multistep process initiated by peptide adsorption to the intact membrane, primarily governed by electrostatic attractions, and followed by peptide insertion [66]. Pep-1 is known to translocate lipid membranes via a physically driven mechanism associated to the high affinity for the phospholipid head groups [66].

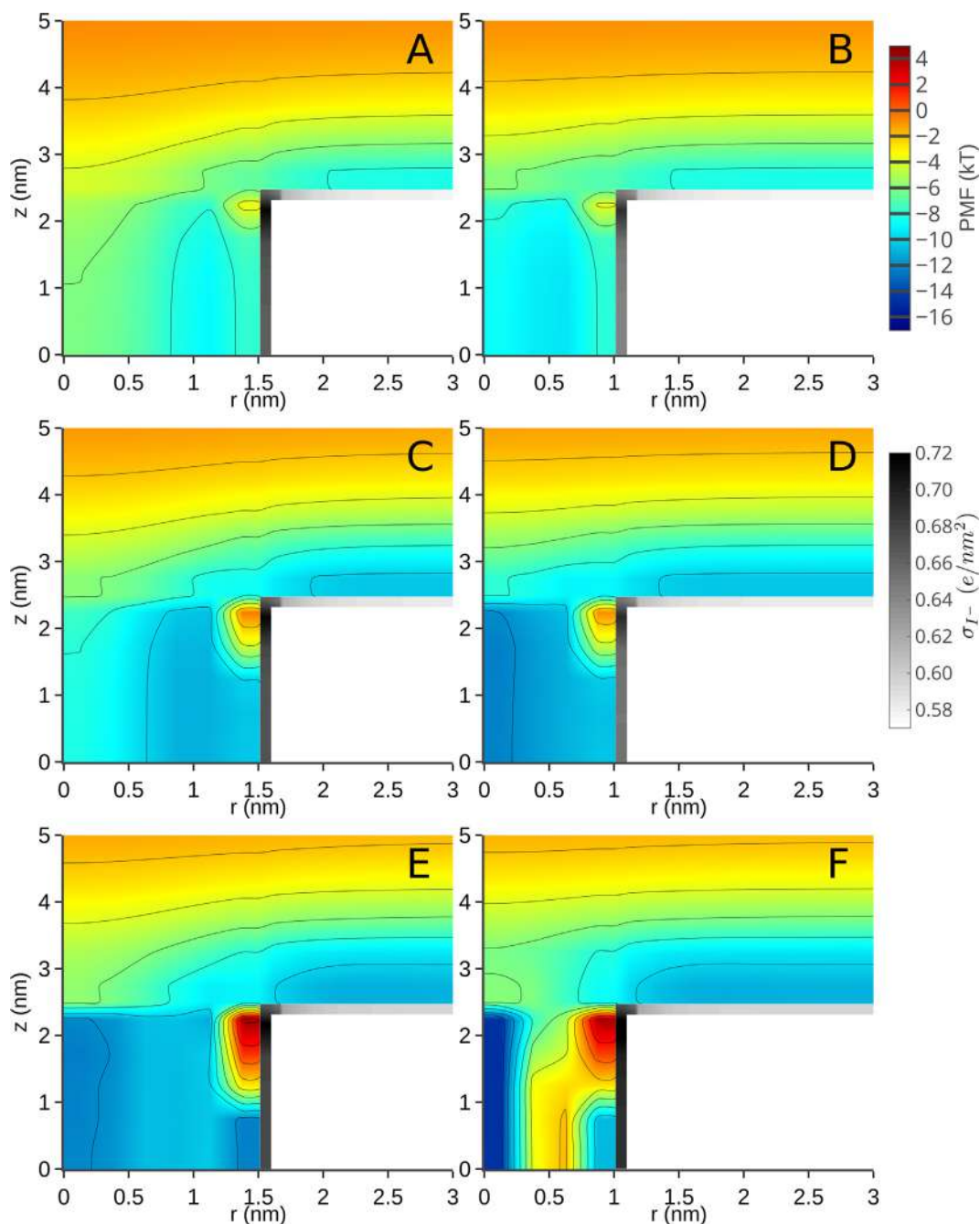


Fig. 7. Color maps showing the potential of mean force acting on a peptide as function of position, (r, z) , for different peptide sizes and pore radii. Panels in the same line correspond to the same peptide chain length, while columns correspond to the same pore radius; A: $L = 4, R = 1.5$ nm; B: $L = 4, R = 1$ nm; C: $L = 6, R = 1.5$ nm; D: $L = 6, R = 1$ nm; E: $L = 9, R = 1.5$ nm; F: $L = 9, R = 1$ nm. The gray-scale placed on the membrane surface gives σ_T , the local charge density on the membrane surface. (For interpretation of the references to color in this figure legend, the reader is referred to the web version of this article.)

As we have seen, when a peptide approaches a porated membrane from the bulk solution, the minimum free energy path takes it first to the surface, and introduces it into the pore in a second stage (see Fig. 6 and Fig. 7). This second mechanistic step involves the nucleation of a hydrophilic pore as the peptide moves across the bilayer. The passive translocation of the peptide can thus be modeled in terms of three coupled first-order kinetic processes, as represented in the following reactions' scheme:



The CPP approaches the “outer” membrane leaflet from a bulk solution of concentration ρ_p^b , while the “inner” leaflet is contact with a solution where $\rho_p^b = 0$ (intra-cellular space). The first two processes in Eq. (10) correspond to the adsorption/desorption of the CPP on/from the membrane surface, which we consider to be in dynamical equilibrium and characterized by the equilibrium constant $K_{\text{ads}} = \rho_p^{\text{mem}} / \rho_p^b = e^{-\beta \Delta F_{\text{ads}}}$, where ρ_p^{mem} is the peptide concentration on the membrane surface at the position of the local minimum of $PMF(r, z)$ and ΔF_{ads} is the adsorption free energy on the intact surface.

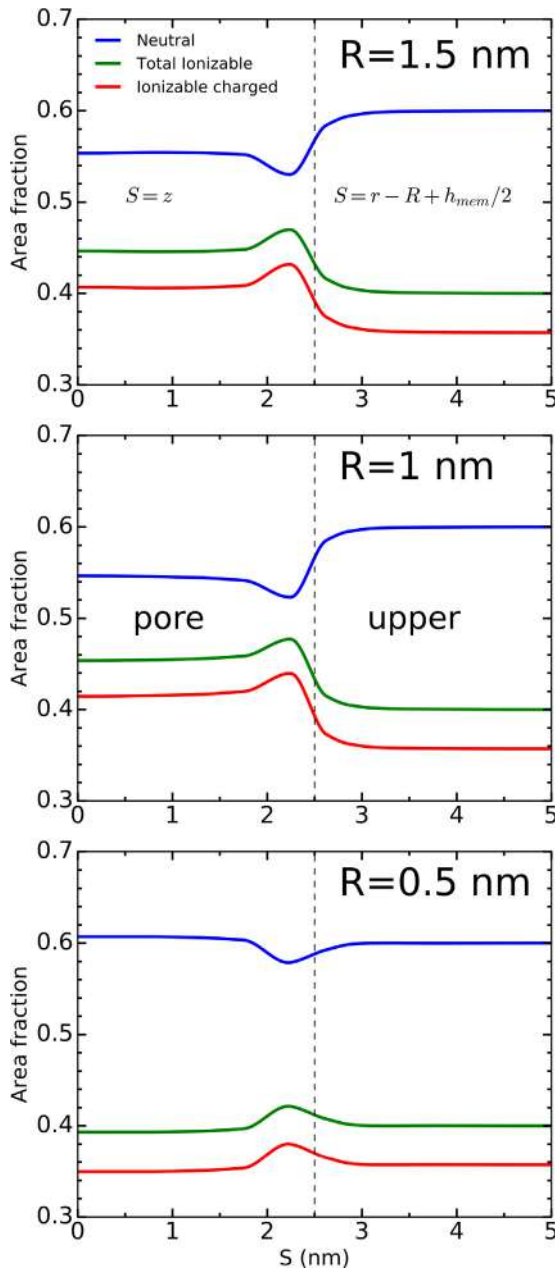


Fig. 8. Local area fraction occupied by different lipid species as a function of the surface coordinate, S , for ARG_9 solutions and membranes having pores of 1.5 nm, 1 nm and 0.5 nm. The blue lines correspond to the charge neutral lipid and the green lines to the acidic lipid (including both the protonated and the deprotonated states). The red lines represent the contribution from the charged (deprotonated acidic) lipids, which is proportional to the membrane charge density (in absolute value). Dashed lines indicate the position of the edge where increasing S results in moving from the pore (cylindrical) surface to the upper membrane (planar) surface. (For interpretation of the references to colour in this figure legend, the reader is referred to the web version of this article.)

The third stage of this mechanism corresponds to the thermally activated jump of the CPP across the bilayer, occurring at a rate $v_t = -k_t \rho_p^{mem}$, with k_t given by Arrhenius equation $k_t = \alpha e^{-\beta \Delta F_{act}}$. As supported by molecular simulations [47,54], the passage of the peptide across the membrane occurs in concert with the opening of a hydrophilic membrane pore, and the kinetic bottleneck occurs when the peptide reaches the center of the bilayer, surmounting an activation barrier ΔF_{act} . Putting the previous equations together, the translocation rate can be written as:

$$v_t = -\alpha \rho_p^b \exp(-\beta \Delta F_{ins}) \quad (11)$$

where $\Delta F_{ins} = \Delta F_{ads} + \Delta F_{act}$ is the cost of inserting the CPP in the bilayer, starting from the bulk solution, while nucleating a transmembrane pore; α is a pre-exponential factor. Eq. (11) shows that the flux of CPP across the membrane is affected, if not determined, by the competition between the binding strength to the membrane surface and the penalty for creating the transition state.

As stated before, our molecular theory model considers the membrane to be a dielectric continuum with titratable surface sites (with translational freedom). Consequently, the model does not account for all the molecular complexities involved in nucleating a transmembrane hydrophilic pore, such as local mechanical deformation, lipids reorientation, membrane pinching, and pore hydration. Instead, we consider that the cost of creating the pore is given by the standard phenomenological expression for the pore-nucleation free energy, when a pore of radius R opens in a membrane under zero lateral tension [67–71]:

$$\Delta F_{pheno}(R) = 2\pi R\gamma + \Delta F_{nuc} \quad (12)$$

where ΔF_{nuc} is the pore nucleation free energy and γ is the membrane line tension. Using this expression we can estimate the pore-radius dependent insertion free energy as,

$$\Delta F_{ins}(R) = \Delta F_{ads} + \Delta F_{pheno}(R) + \Delta PMF \quad (13)$$

where $\Delta F_{pheno} + \Delta PMF \approx \Delta F_{act}$, and $\Delta PMF = PMF_{pore} - PMF_{mem}$ is the free energy change (computed with our model) when the peptide moves from the membrane surface into the pore (once the pore has been created). In other words, PMF_{mem} is the value of the potential of mean force at the surface of the intact membrane, and PMF_{pore} corresponds to the value of the global minimum of $PMF(r, z)$. Notice that PMF_{mem} is not significantly different from the minimum of the PMF constrained to the upper membrane surface ($z = \frac{h_{mem}}{2}$). It is also important to emphasize that, as with any change in thermodynamic variables, ΔF_{act} can be computed as the sum of two separate contributions: the pore formation energy, and the cost of moving the peptide from the surface of the membrane to the pore interior. This does not mean that the jump of the CPP across the bilayer occurs in two consecutive stages, *i.e.*, pore opening followed by peptide diffusion through or into the pore. In fact, molecular dynamics simulations have shown that pore opening and peptide crossing occur in a concerted way until the transition state configuration is reached. It is the energy of such configuration, in which the peptide seats inside a hydrated membrane pore, that can be computed from Eq. (13).

Fig. 9 shows ΔPMF as a function of the peptide chain length for different pore sizes. Clearly, in all cases, there is small free energy decrease when the peptide moves from the surface to the pore interior; *i.e.*, peptide insertion slightly stabilizes the porated membrane. However, this free energy gain is overwhelmed by the cost of creating the pore. For example, Table 1 reports the values of ΔF_{pheno} calculated using standard values of $\Delta F_{nuc} = 200$ kJ/mol and membrane line tension $\gamma = 40$ pN [71], for the pore radii considered in Fig. 9. When comparing the values presented in this table with the results of Fig. 9, we see that the cost of opening a pore is significantly larger than the gain upon insertion of one peptide (roughly two orders of magnitude), even if we consider the best case scenario of 1.5 ARG_9 molecules inserting into a 1 nm radius pore (see Fig. 5). In other words, the translocation of the peptide starting from the membrane surface is uphill in free energy, as expected for an activated process ($\Delta F_{act} > 0$), and shows an activation barrier of the order of hundreds of $k_B T$. Such a large translocation barrier coincides in the order of magnitude with the ones computed by molecular dynamics simulations for most CPPs [46,47,51–56].

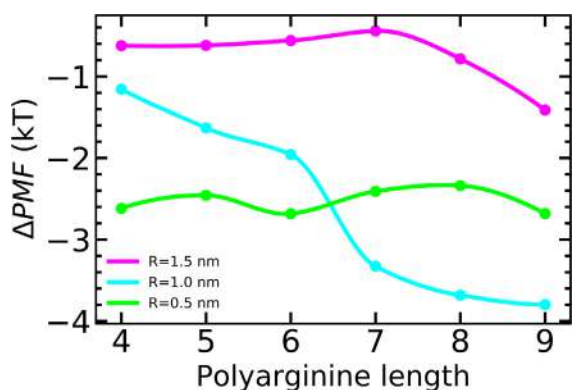


Fig. 9. Free energy change when a peptide moves from the upper membrane surface to the pore interior, as a function of peptide chain length for different pore radii. These results have been obtained at physiological conditions (pH 7 and 0.1 M NaCl) and peptide concentration 1 μ M.

Table 1

Free energy cost of pore opening within the standard phenomenological pore-nucleation model.

R, (nm)	$\Delta F_{\text{pheno.}}$ ($k_B T$)
0.5	111.4
1.0	141.7
1.5	172.1

In light of our results, Eq. (11) informs us that the peptides' absolute translocation rate could be more effectively modulated by controlling the factors that determine the adsorption energy, rather than trying to diminish the penalizing effect of ΔF_{act} . On the other hand, the relative translocation efficiency of structurally different CPPs, $e_{\text{rel}} = v_t^{\text{CPP}_1} / v_t^{\text{CPP}_2}$, may well be affected by both adsorption and activation energies. The theoretical approach presented in this paper may help unraveling the molecular properties that make some CPPs more effective than others.

4. Conclusions

We have developed a molecular theory to investigate the adsorption and insertion of arginine peptides into membrane pores. This method, which incorporates the explicit description of peptide size, shape and conformations as well as lipid membrane charge regulation, allows for a systematic investigation of the effects of pore size, peptide concentration and sequence length.

Our results indicate that adsorption to the intact lipid membrane plays a critical role on peptide translocation; *i.e.*, peptide pre-concentrates on the membrane surface before jumping across the membrane. For peptides shorter than AR_{G_9} , adsorption on the intact membrane increases significantly with chain length. For longer CPPs, however, the adsorption extent does not considerably increase with peptide length. This behavior holds for the typical experimental conditions of low peptide concentrations. Increasing the peptide concentration, on the other hand, favors the adsorption of shorter sequences.

Adsorption into the pore displays a non-monotonic dependence on pore size, which is due to the short range nature of the effective membrane-peptide interactions. Maximum adsorption into the pore occurs when the pore radius is around 1 nm, but this effect is modulated by the peptide chain length.

The negative charge on the membrane surface increases with peptide chain length (intact membrane), which results exclusively from a lower degree of protonation of acidic lipids. In addition, the

pore surface is more negatively charged than the upper membrane surface under most conditions. This effect, on the other hand, is a consequence of the exchange between neutral and (charged) acidic lipids, without altering the local degree of protonation. These charge-regulation phenomena enhance the attractive electrostatic lipid-peptide interaction, which provides the driving force for adsorption. The translational freedom of the lipids has a bigger impact on the surface charge density than the possibility of displacing the acid-base chemical equilibrium of the titratable lipids. In this context, the size of the pore has an important effect on the surface charge density inside the pore, while the effect of peptide chain-length is less significant.

Biological membranes have a wide range of lipid compositions [72]. It has been shown, for example, that lipid clustering can cause dramatic changes in local membrane composition [73]. Here, we have studied a membrane composed of 60% neutral lipid and 40% acidic lipid. At the present, we are conducting further research to study the role of membrane composition on peptide adsorption and translocation.

We have considered the adsorption of polycationic CPPs driven by electrostatic attractions. These attractions alone do not provide the free energy gain to offset the cost of opening a hydrophilic pore. In other words, CPPs' translocation is uphill in free-energy, as expected for a thermally activated process. A simple kinetic model highlights the role of adsorption, pore nucleation, and peptide insertion energies. While the absolute translocation rate of a peptide is dominated by the energy cost of creating a peptide-filled trans-membrane pore, electrostatically driven adsorption on the intact membrane provides a large population of peptides ready to jump across the membrane. Our results indicate that a reasonable approach in the rational design of efficient CPPs should focus on enhancing membrane adsorption, rather than diminishing the penalty of membrane crossing.

The theoretical approach presented in this paper should allow to investigate the relative translocation efficiency of structurally different CPPs, by comparing their membrane insertion free energies as defined in equation Eq. (11). For example, the presence of neutral (hydrophobic) residues in the amino acid sequence, intercalated between charged ones, can increase the CPP's translocation rate [74–76]. In this sense, Thryptophan seems to be a particularly good neutral spacer [77,75]. We are currently extending our model to describe amphipathic peptides and address the relative translocation efficiency of different CPPs.

Acknowledgements

This work was supported by CONICET and ANPCyT (PICT-2014-3377, PICT-2017-3513), Argentina. M.G.D.P. acknowledges financial support from CONICET, SECTyP-UNCUYO and ANPCyT (PICT-2015-1835), and J.A.V. from CONICET (PIP-0087), UNSL (PROICO 3-2212) and ANPCyT (PICT-2014-0556, PICT-2015-0767), Argentina. I.S. acknowledges support from NSF, Div. of Chem., Bioeng., Env., & Transp. Sys. 1833214. M.G.D.P. thanks Prof. L. S. Mayorga for useful discussions.

Appendix A. Supplementary material

Supplementary data associated with this article can be found, in the online version, at <https://doi.org/10.1016/j.jcis.2019.05.087>.

References

- [1] S. El-Andaloussi, T. Holm, U. Langel, Cell-penetrating peptides: mechanisms and applications, *Curr. Pharm. Des.* 11 (28) (2005) 3597–3611.
- [2] H. Ti Tien, Diana A. Louise, Bimolecular lipid membranes: A review and a summary of some recent studies, *Chem. Phys. Lipids* 2 (1) (1968) 55–101.

- [https://doi.org/10.1016/0009-3084\(68\)90035-2](https://doi.org/10.1016/0009-3084(68)90035-2). <http://www.sciencedirect.com/science/article/pii/S0009308468900352>.
- [3] S.R. Schwarze, A. Ho, A. Vocero-Akbani, S.F. Dowdy, In vivo protein transduction: delivery of a biologically active protein into the mouse, *Science (New York, NY)* 285 (5433) (1999) 1569–1572.
- [4] S. Futaki, Membrane-permeable arginine-rich peptides and the translocation mechanisms, *Adv. Drug Deliv. Rev.* 57 (4) (2005) 547–558, <https://doi.org/10.1016/j.addr.2004.10.009>. <http://www.sciencedirect.com/science/article/pii/S0169409X0400273X>.
- [5] M. Zorko, U. Langel, Cell-penetrating peptides: mechanism and kinetics of cargo delivery, *Adv. Drug Deliv. Rev.* 57 (4) (2005) 529–545, <https://doi.org/10.1016/j.addr.2004.10.010>.
- [6] F. Heitz, M.C. Morris, G. Divita, Twenty years of cell-penetrating peptides: from molecular mechanisms to therapeutics, *Br. J. Pharmacol.* 157 (2) (2009) 195–206, <https://doi.org/10.1111/j.1476-5381.2009.00057.x>.
- [7] A. El-Sayed, S. Futaki, H. Harashima, Delivery of macromolecules using arginine-rich cell-penetrating peptides: ways to overcome endosomal entrapment, *AAPS J* 11 (1) (2009) 13–22, <https://doi.org/10.1208/s12248-008-9071-2>.
- [8] P. Ruzza, B. Biondi, A. Marchiani, N. Antolini, A. Calderan, Cell-Penetrating Peptides: A Comparative Study on Lipid Affinity and Cargo Delivery Properties, *Pharmaceuticals (Basel, Switzerland)* 3 (4) (2010) 1045–1062, <https://doi.org/10.3390/ph3041045>.
- [9] F. Mussbach, M. Franke, A. Zoch, B. Schaefer, S. Reissmann, Transduction of peptides and proteins into live cells by cell penetrating peptides, *J. Cell. Biochem.* 112 (12) (2011) 3824–3833, <https://doi.org/10.1002/jcb.23313>.
- [10] J. Hoyer, I. Neundorff, Peptide vectors for the nonviral delivery of nucleic acids, *Acc. Chem. Res.* 45 (7) (2012) 1048–1056, <https://doi.org/10.1021/ar2002304>.
- [11] E. Koren, V.P. Torchilin, Cell-penetrating peptides: breaking through to the other side, *Trends Mol. Med.* 18 (7) (2012) 385–393, <https://doi.org/10.1016/j.molmed.2012.04.012>.
- [12] C. Bechara, S. Sagan, Cell-penetrating peptides: 20 years later, where do we stand?, *FEBS Lett* 587 (12) (2013) 1693–1702, <https://doi.org/10.1016/j.febslet.2013.04.031>.
- [13] M.C. Shin, J. Zhang, K.A. Min, K. Lee, Y. Byun, A.E. David, et al., Cell-penetrating peptides: achievements and challenges in application for cancer treatment, *J. Biomed. Mater. Res. Part A* 102 (2) (2014) 575–587, <https://doi.org/10.1002/jbm.a.34859>.
- [14] S.M. Farkhani, A. Valizadeh, H. Karami, S. Mohammadi, N. Sohrabi, F. Badrzadeh, Cell penetrating peptides: efficient vectors for delivery of nanoparticles, nanocarriers, therapeutic and diagnostic molecules, *Peptides* 57 (2014) 78–94, <https://doi.org/10.1016/j.peptides.2014.04.015>.
- [15] M. Di Pisa, G. Chassaing, J.M. Swiecicki, Translocation Mechanism(s) of Cell-Penetrating Peptides: Biophysical Studies Using Artificial Membrane Bilayers, *Biochemistry* 54 (2) (2015) 194–207, <https://doi.org/10.1021/bi501392n>.
- [16] S. Zappavigna, G. Misso, A. Falanga, E. Perillo, E. Novellino, M. Galdiero, et al., Nanocarriers Conjugated with Cell Penetrating Peptides: New Trojan Horses by Modern Ulysses, *Curr. Pharm. Biotechnol.* 17 (8) (2016) 700–722.
- [17] A. Dinca, W.M. Chien, M.T. Chin, Intracellular delivery of proteins with cell-penetrating peptides for therapeutic uses in human disease, *Int. J. Mol. Sci.* 17 (2) (2016) 263, <https://doi.org/10.3390/ijms17020263>.
- [18] L. Pan, Q. He, J. Liu, Y. Chen, M. Ma, L. Zhang, et al., Nuclear-targeted drug delivery of TAT peptide-conjugated monodisperse mesoporous silica nanoparticles, *J. Am. Chem. Soc.* 134 (13) (2012) 5722–5725, <https://doi.org/10.1021/ja211035w>.
- [19] Y. Fukuoka, E.S. Khafagy, T. Goto, N. Kamei, K. Takayama, N.A. Peppas, et al., Combination Strategy with Complexation Hydrogels and Cell-Penetrating Peptides for Oral Delivery of Insulin, *Biol. Pharmaceut. Bull.* 41 (5) (2018) 811–814, <https://doi.org/10.1248/bpb.b17-00951>.
- [20] A.D. Frankel, C.O. Pabo, Cellular uptake of the tat protein from human immunodeficiency virus, *Cell* 55 (6) (1988) 1189–1193.
- [21] J.L. Lau, M.K. Dunn, Therapeutic peptides: Historical perspectives, current development trends, and future directions, *Bioorganic Med. Chem.* 26 (10) (2018) 2700–2707, <https://doi.org/10.1016/j.bmc.2017.06.052>. URL <http://www.sciencedirect.com/science/article/pii/S0968089617310222>.
- [22] A.L. Lewis, J. Richard, Challenges in the delivery of peptide drugs: an industry perspective, *Therapeutic Deliv.* 6 (2) (2015) 149–163, <https://doi.org/10.4155/tde.14.111>. <http://www.future-science.com/doi/10.4155/tde.14.111>.
- [23] A. Chugh, F. Eudes, Y.S. Shim, Cell-penetrating peptides: Nanocarrier for macromolecule delivery in living cells, *IUBMB Life* 62 (3) (2010) 183–193, <https://doi.org/10.1002/iub.297>.
- [24] E. Vivès, P. Brodin, B. Lebleu, A truncated HIV-1 Tat protein basic domain rapidly translocates through the plasma membrane and accumulates in the cell nucleus, *J. Biol. Chem.* 272 (25) (1997) 16010–16017.
- [25] P.A. Wender, D.J. Mitchell, K. Pattabiraman, E.T. Pelkey, L. Steinman, J.B. Rothbard, The design, synthesis, and evaluation of molecules that enable or enhance cellular uptake: peptidic molecular transporters, *Proc. Nat. Acad. Sci. USA* 97 (24) (2000) 13003–13008, <https://doi.org/10.1073/pnas.97.24.13003>.
- [26] G. Drin, M. Mazel, P. Clair, D. Mathieu, M. Kaczorek, J. Tamsamani, Physicochemical requirements for cellular uptake of pAntp peptide. Role of lipid-binding affinity, *Eur. J. Biochem.* 268 (5) (2001) 1304–1314.
- [27] A. Ziegler, X.L. Blatter, A. Seelig, J. Seelig, Protein transduction domains of HIV-1 and SIV TAT interact with charged lipid vesicles. Binding mechanism and thermodynamic analysis, *Biochemistry* 42 (30) (2003) 9185–9194, <https://doi.org/10.1021/bi0346805>.
- [28] A. Ziegler, Thermodynamic studies and binding mechanisms of cell-penetrating peptides with lipids and glycosaminoglycans, *Adv. Drug Deliv. Rev.* 60 (4) (2008) 580–597, <https://doi.org/10.1016/j.addr.2007.10.005>. <http://www.sciencedirect.com/science/article/pii/S0169409X0700292X>.
- [29] Y. Takechi, H. Yoshii, M. Tanaka, T. Kawakami, S. Aimoto, H. Saito, Physicochemical mechanism for the enhanced ability of lipid membrane penetration of polyarginine, *Langmuir* 27 (11) (2011) 7099–7107, <https://doi.org/10.1021/la200917y>. URL <http://pubs.acs.org/doi/abs/10.1021/la200917y>.
- [30] N. Schmidt, A. Mishra, G.H. Lai, G.C.L. Wong, Arginine-rich cell-penetrating peptides, *FEBS Lett.* 584 (9) (2010) 1806–1813, <https://doi.org/10.1016/j.febslet.2009.11.046>.
- [31] H.L. Åmand, H.A. Rydberg, L.H. Fornander, P. Lincoln, B. Nordén, E.K. Esbjörner, Cell surface binding and uptake of arginine- and lysine-rich penetratin peptides in absence and presence of proteoglycans, *Biochimica et Biophysica Acta (BBA) - Biomembranes* 1818 (11) (2012) 2669–2678, <https://doi.org/10.1016/j.bbame.2012.06.006>. URL <http://www.sciencedirect.com/science/article/pii/S0005273612001940>.
- [32] P.E.G. Thorén, D. Persson, E.K. Esbjörner, M. Goksör, P. Lincoln, B. Nordén, Membrane binding and translocation of cell-penetrating peptides, *Biochemistry* 43 (12) (2004) 3471–3489, <https://doi.org/10.1021/bi0360049>.
- [33] W.B. Kauffman, T. Fuselier, J. He, W.C. Wimley, Mechanism matters: A taxonomy of cell penetrating peptides, *Trends Biochem. Sci.* 40 (12) (2015) 749–764, <https://doi.org/10.1016/j.tibs.2015.10.004>. <https://www.ncbi.nlm.nih.gov/pmc/articles/PMC4727446/>.
- [34] S. Deshayes, A. Heitz, M.C. Morris, P. Charnet, G. Divita, F. Heitz, Insight into the mechanism of internalization of the cell-penetrating carrier peptide Pep-1 through conformational analysis, *Biochemistry* 43 (6) (2004) 1449–1457, <https://doi.org/10.1021/bi035682s>.
- [35] C.Y. Jiao, D. Delaroché, F. Burlina, I.D. Alves, G. Chassaing, S. Sagan, Translocation and endocytosis for cell-penetrating peptide internalization, *J. Biol. Chem.* 284 (49) (2009) 33957–33965, <https://doi.org/10.1074/jbc.M109.056309>.
- [36] A. Walrant, I. Correia, C.Y. Jiao, O. Lequin, E.H. Bent, N. Goasdoué, et al., Different membrane behaviour and cellular uptake of three basic arginine-rich peptides, *Biochim. Biophys. Acta* 1808 (1) (2011) 382–393, <https://doi.org/10.1016/j.bbame.2010.09.009>.
- [37] D. Derossi, A.H. Joliot, G. Chassaing, A. Prochiantz, The third helix of the Antennapedia homeodomain translocates through biological membranes, *J. Biol. Chem.* 269 (14) (1994) 10444–10450.
- [38] E. Vivès, J.P. Richard, C. Rispal, B. Lebleu, TAT peptide internalization: seeking the mechanism of entry, *Curr. Protein Peptide Sci.* 4 (2) (2003) 125–132.
- [39] H.D. Herce, A.E. Garcia, Cell penetrating peptides: How Do They Do It? *J. Biol. Phys.* 33 (5–6) (2007) 345–356, <https://doi.org/10.1007/s10867-008-9074-3>. <https://www.ncbi.nlm.nih.gov/pmc/articles/PMC2565759/>.
- [40] Y. Pouny, D. Rapoport, A. Mor, P. Nicolas, Y. Shai, Interaction of antimicrobial dermaseptin and its fluorescently labeled analogs with phospholipid membranes, *Biochemistry* 31 (49) (1992) 12416–12423, <https://doi.org/10.1021/bi00164a017>. URL <http://pubs.acs.org/doi/abs/10.1021/bi00164a017>.
- [41] D. Derossi, S. Calvet, A. Trembleau, A. Brunissen, G. Chassaing, A. Prochiantz, Cell internalization of the third helix of the antennapedia homeodomain is receptor-independent, *J. Biol. Chem.* 271 (30) (1996) 18188–18193, <https://doi.org/10.1074/jbc.271.30.18188>. URL <http://www.jbc.org/content/271/30/18188>.
- [42] K. Matsuzaki, S. Yoneyama, O. Murase, K. Miyajima, Transbilayer transport of ions and lipids coupled with Mastoparan X translocation, *Biochemistry* 35 (25) (1996) 8450–8456, <https://doi.org/10.1021/bi960342a>.
- [43] F. Madani, S. Lindberg, U. Langel, S. Futaki, A. Gräslund, Mechanisms of cellular uptake of cell-penetrating peptides, *J. Biophys. (Hindawi Publishing Corporation: Online)* 2011 (2011) 414729, <https://doi.org/10.1155/2011/414729>.
- [44] D. Sun, J. Forsman, M. Lund, C.E. Woodward, Effect of arginine-rich cell penetrating peptides on membrane pore formation and life-times: a molecular simulation study, *Phys. Chem. Chem. Phys.* 16 (38) (2014) 20785–20795, <https://doi.org/10.1039/C4CP02211D>. URL <https://pubs.rsc.org/en/content/articlelanding/2014/cp/c4cp02211d>.
- [45] J. Ye, E. Liu, Z. Yu, X. Pei, S. Chen, P. Zhang, et al., CPP-assisted intracellular drug delivery, What Is Next?, *Int. J. Mol. Sci.* 17 (11) (2016) 1892, <https://doi.org/10.3390/ijms17111892>. <https://www.ncbi.nlm.nih.gov/pmc/articles/PMC5133891/>.
- [46] H.D. Herce, A.E. Garcia, J. Litt, R.S. Kane, P. Martin, N. Enrique, et al., Arginine-rich peptides destabilize the plasma membrane, consistent with a pore formation translocation mechanism of cell penetrating peptides, *Biophys. J.* 97 (7) (2009) 1917–1925, <https://doi.org/10.1016/j.bpj.2009.05.066>. arXiv: 0910.1736. <http://arxiv.org/abs/0910.1736>.
- [47] M.A. Via, J. Klug, N. Wilke, L.S. Mayorca, M.G. Del Pópolo, The interfacial electrostatic potential modulates the insertion of cell-penetrating peptides into lipid bilayers, *Phys. Chem. Chem. Phys.* 20 (7) (2018) 5180–5189, <https://doi.org/10.1039/C7CP07243K>.
- [48] A.T. Jones, E.J. Sayers, Cell entry of cell penetrating peptides: tales of tails wagging dogs, *J. Controlled Release* 161 (2) (2012) 582–591, <https://doi.org/10.1016/j.jconrel.2012.04.003>. <http://www.sciencedirect.com/science/article/pii/S0168365912002441>.
- [49] A. Komin, L.M. Russell, K.A. Hristova, P.C. Seanson, Peptide-based strategies for enhanced cell uptake, transcellular transport, and circulation: Mechanisms and challenges, *Adv. Drug Deliv. Rev.* 110–111 (2017) 52–64, <https://doi.org/10.1016/j.addr.2016.06.002>.

- [50] J.L. Zaro, W.C. Shen, Cationic and amphipathic cell-penetrating peptides (CPPs): Their structures and in vivo studies in drug delivery, *Front. Chem. Sci. Eng.* 9 (4) (2015) 407–427, <https://doi.org/10.1007/s11705-015-1538-y>.
- [51] Li Zi, H.m. Ding, Y.q. Ma, Translocation of polyarginines and conjugated nanoparticles across asymmetric membranes, *Soft Matter* 9 (4) (2012) 1281–1286, <https://doi.org/10.1039/C2SM26519B>. URL <http://pubs.rsc.org/en/content/articlelanding/2013/sm/c2sm26519b>.
- [52] D. Sun, J. Forsman, C.E. Woodward, Atomistic molecular simulations suggest a kinetic model for membrane translocation by arginine-rich peptides, *J. Phys. Chem. B* 119 (45) (2015) 14413–14420, <https://doi.org/10.1021/acs.jpcc.5b08072>.
- [53] B. Sha, F. Xu, M. Lin, S. Feng, X. He, X. Shi, et al., Coarse-grained molecular dynamics studies of the translocation mechanism of polyarginines across asymmetric membrane under tension, *Sci. Rep.* 5 (2015) srep12808, <https://doi.org/10.1038/srep12808>. <https://www.nature.com/articles/srep12808>.
- [54] Y. Hu, S. Patel, Thermodynamics of cell-penetrating HIV1 TAT peptide insertion into PC/PS/CHOL model bilayers through transmembrane pores: the roles of cholesterol and anionic lipids, *Soft Matter* 12 (32) (2016) 6716–6727, <https://doi.org/10.1039/c5sm01696g>.
- [55] X.C. He, Z.G. Qu, F. Xu, Simulation study of interaction mechanism between peptide and asymmetric membrane, *Mol. Simul.* 43 (1) (2017) 34–41, <https://doi.org/10.1080/08927022.2016.1228105>.
- [56] J. Klug, D. Mason, M.G.D. Pópolo, Molecular-level insight into the binding of arginine to a zwitterionic Langmuir monolayer, *RSC Adv* 7 (49) (2017) 30862–30869, <https://doi.org/10.1039/C7RA05359B>. URL <https://pubs.rsc.org/en/content/articlelanding/2017/ra/c7ra05359b>.
- [57] D.J. Mitchell, D.T. Kim, L. Steinman, C.G. Fathman, J.B. Rothbard, Polyarginine enters cells more efficiently than other polycationic homopolymers, *J. Peptide Res.: Off. J. Am. Peptide Soc.* 56 (5) (2000) 318–325.
- [58] W. Dowhan, Molecular basis for membrane phospholipid diversity: Why Are There So Many Lipids?, *Annu. Rev. Biochem.* 66 (1) (1997) 199–232, <https://doi.org/10.1146/annurev.biochem.66.1.199>.
- [59] R.B. Gennis, *Biomembranes: Molecular Structure and Function*, Springer, 2013. ISBN 978-1-4757-2065-5. Google-Books-ID: RjBkBWAAQBAJ.
- [60] D. Schmidt, Q.X. Jiang, R. MacKinnon, Phospholipids and the origin of cationic gating charges in voltage sensors, *Nature* 444 (7120) (2006) 775–779, <https://doi.org/10.1038/nature05416>. <https://www.nature.com/articles/nature05416>.
- [61] S. Li, Y. Su, W. Luo, M. Hong, Water-protein interactions of an arginine-rich membrane peptide in lipid bilayers investigated by solid-state nuclear magnetic resonance spectroscopy, *J. Phys. Chem. B* 114 (11) (2010) 4063–4069, <https://doi.org/10.1021/jp912283r>.
- [62] F.J. Millero, A. Lo Surdo, C. Shin, The apparent molal volumes and adiabatic compressibilities of aqueous amino acids at 25.degree.C, *J. Phys. Chem.* 82 (7) (1978) 784–792, <https://doi.org/10.1021/j100496a007>. <http://pubs.acs.org/doi/abs/10.1021/j100496a007>.
- [63] P.J. Flory, *Statistical Mechanics of Chain Molecules*, Interscience Publishers, 1969. Google-Books-ID: EDZRAAAAMAAJ.
- [64] A.L. Becker, K. Henzler, N. Welsch, M. Ballauff, O. Borisov, Proteins and polyelectrolytes: A charged relationship, *Curr. Opin. Colloid Interface Sci.* 17 (2) (2012) 90–96, <https://doi.org/10.1016/j.cocis.2011.10.001>. <http://www.sciencedirect.com/science/article/pii/S1359029411001294>.
- [65] J.J. López Cascales, S. Zenak, J. García de la Torre, O.G. Lezama, A. Garro, R.D. Enriz, Small cationic peptides: influence of charge on their antimicrobial activity, *ACS Omega* 3 (5) (2018) 5390–5398, <https://doi.org/10.1021/acsomega.8b00293>.
- [66] S.T. Henriques, M.A.R.B. Castanho, L.K. Pattenden, M.I. Aguilar, Fast membrane association is a crucial factor in the peptide pep-1 translocation mechanism: A kinetic study followed by surface plasmon resonance, *Pept. Sci.* 94 (3) (2010) 314–322, <https://doi.org/10.1002/bip.21367>. <https://www.onlinelibrary.wiley.com/doi/abs/10.1002/bip.21367>.
- [67] T.V. Tolpekina, W.K. den Otter, W.J. Briels, Nucleation free energy of pore formation in an amphiphilic bilayer studied by molecular dynamics simulations, *J. Chem. Phys.* 121 (23) (2004) 12060–12066, <https://doi.org/10.1063/1.1815296>.
- [68] Z.J. Wang, D. Frenkel, Pore nucleation in mechanically stretched bilayer membranes, *J. Chem. Phys.* 123 (15) (2005) 154701, <https://doi.org/10.1063/1.2060666>.
- [69] J. Wohler, W.K. den Otter, O. Edholm, W.J. Briels, Free energy of a transmembrane pore calculated from atomistic molecular dynamics simulations, *J. Chem. Phys.* 124 (15) (2006) 154905, <https://doi.org/10.1063/1.2171965>.
- [70] W.K. den Otter, Free energies of stable and metastable pores in lipid membranes under tension, *J. Chem. Phys.* 131 (20) (2009) 205101, <https://doi.org/10.1063/1.3266839>.
- [71] J.M.L. Martí, N.J. English, M.G.D. Pópolo, Elucidating mysteries of phase-segregated membranes: mobile-lipid recruitment facilitates pores' passage to the fluid phase, *Phys. Chem. Chem. Phys.* 20 (28) (2018) 19234–19239, <https://doi.org/10.1039/C8CP00958A>. URL <https://pubs.rsc.org/en/content/articlelanding/2018/cp/c8cp00958a>.
- [72] S.E. Horvath, G. Daum, Lipids of mitochondria, *Prog. Lipid Res.* 52 (4) (2013) 590–614, <https://doi.org/10.1016/j.plipres.2013.07.002>. <http://linkinghub.elsevier.com/retrieve/pii/S0163782713000519>.
- [73] P. Wadhvani, R. Epanand, N. Heidenreich, J. Bürck, A. Ulrich, Membrane-active peptides and the clustering of anionic lipids, *Biophys. J.* 103 (2) (2012) 265–274, <https://doi.org/10.1016/j.bpj.2012.06.004>. <https://www.ncbi.nlm.nih.gov/pmc/articles/PMC3400765/>.
- [74] J.B. Rothbard, E. Kreider, C.L. VanDeusen, L. Wright, B.L. Wylie, P.A. Wender, Arginine-rich molecular transporters for drug delivery: role of backbone spacing in cellular uptake, *J. Med. Chem.* 45 (17) (2002) 3612–3618, <https://doi.org/10.1021/jm0105676>.
- [75] H.A. Rydberg, M. Matson, H.L. Åmand, E.K. Esbjörner, B. Nordén, Effects of tryptophan content and backbone spacing on the uptake efficiency of cell-penetrating peptides, *Biochemistry* 51 (27) (2012) 5531–5539, <https://doi.org/10.1021/bi300454k>.
- [76] G. Lättig-Tünnemann, M. Prinz, D. Hoffmann, J. Behlke, C. Palm-Apergi, I. Morano, et al., Backbone rigidity and static presentation of guanidinium groups increases cellular uptake of arginine-rich cell-penetrating peptides, *Nat. Commun.* 2 (2011) 453, <https://doi.org/10.1038/ncomms1459>.
- [77] D.I. Chan, E.J. Prenner, H.J. Vogel, Tryptophan- and arginine-rich antimicrobial peptides: structures and mechanisms of action, *Biochim. Biophys. Acta* 1758 (9) (2006) 1184–1202, <https://doi.org/10.1016/j.bbmem.2006.04.006>.